EFFECT OF LBO-SEEDED IMPURITY ON ELMS IN THE HL-2A TOKAMAK

Y.P. Zhang[1,a)], D. Mazon[2,b)], X.L. Zou[2], W.L. Zhong[1], J.M. Gao[1], K. Zhang[1], P. Sun[1], C.F. Dong[1], Z.Y. Cui[1], Yi Liu[1], Z.B. Shi[1], D.L. Yu[1], J. Cheng[1], M. Jiang[1], J.Q. Xu[1], M. Isobe[3,4], G.L. Xiao[1], W. Chen[1], S.D. Song[1], X.Y. Bai[1], P.F. Zhang[1], G.L. Yuan[1], X.Q. Ji[1], Y.G. Li[1], Y. Zhou[1], L. Delpech[2], A. Ekedahl[2], G. Giruzzi[2], T. Hoang[2], Y. Peysson[2], X.M. Song[1], X.Y. Song[1], X.Li[1], X.T. Ding[1], J.Q. Dong[1], Q.W. Yang[1], M. Xu[1], X.R. Duan[1], Y. Liu[1], and the HL-2A team[1]
[1] Southwestern Institute of Physics, Chengdu, China
[2] CEA, IRFM, Saint-Paul-lez-Durance, France
[3] National institute for Fusion Science, Toki, Japan
[4] SOKENDAI, Toki, Japan
E-mail a): zhangyp@swip.ac.cn
E-mail b): didier.mazon@cea.fr

Abstract

Effect of the pedestal deposited impurity on the edge-localized mode (ELM) behaviour has been observed and intensively investigated in the HL-2A tokamak. Impurities have been externally seeded by a newly developed laser blow-off (LBO) system. Both mitigation and suppression of ELMs have been realized by LBO-seeded impurity. Measurements have shown that the LBO-seeded impurity particles are mainly deposited in the pedestal region. During the ELM mitigation phase, the pedestal density fluctuation is significantly increased, indicating that the ELM mitigation may be achieved by the enhancement of the pedestal transport. During the ELM suppression phase, a harmonic coherent mode (HCM) is excited by the LBO-seeded impurity, and the pedestal density fluctuation is significantly decreased, the electron density is continuously increased, implying that HCM may reduce the pedestal turbulence, suppress ELMs, increase the pedestal pressure, thus extending the Peeling-Ballooning instability limit.

1. INTRODUCTION

ELM control has been extensively studied theoretically and experimentally in magnetic fusion devices [1-3]. In order to ensure an appropriate lifetime of PFCs in ITER, it is anticipated that at full plasma current robust ELM control technique will be required, either suppressing the ELMs completely or, at least, reducing the divertor heat flux per ELM. Therefore, there are two primary forms related to the ELM control. The first is ELM mitigation which increases the ELM frequency fELM relative to the intrinsic one whilst at the same time reduces the divertor peak heat flux. Since the relation fELM × ΔWELM ~ constant (here ΔWELM is the energy loss per ELM), holds for intrinsic ELMs on many tokamaks, increasing the fELM should decrease the ΔWELM as we desire. The latter type of ELM control is ELM suppression, which completely avoids the occurrence of large amplitude ELM bursts and simultaneously increases pedestal transport to flush the impurities from the plasma core region by alternative edge instabilities (quasi-coherent modes) rather than the ELMs. Numerous efforts have been dedicated to explore the effective techniques for ELM control and many techniques have been developed. Existing methods for ELM control include resonant magnetic perturbations (RMPs) [4-6], supersonic molecular beam injection (SMBI) [7], small pellet pacing [8], fast vertical jogs of the plasma columns [9], and lower hybrid current drive (LHCD) [10,11].

In this paper, we describe a novel experimental demonstration of ELM control by laser blow-off (LBO) system, and elucidate the physics of the results. Experimental results in several devices suggested that LBO is an effective and well established technique to study impurity transport investigation. In addition to the impurity transport, the effect of LBO injected impurities on the ELM dynamics has been studied in the HL-2A tokamak. Both the mitigation and suppression of the ELMs have been successfully achieved by means of LBO.

2. EXPERIMENTAL CONDITIONS

The HL-2A device is a medium-size tokamak with closed divertor chambers [12]. Its major and minor radii are R = 1.65 m and a = 0.4 m, respectively. The achieved operation parameters are as follows: the plasma current Ip is 450 kA, the toroidal magnetic field at the magnetic axis is 2.7 T, the central line-averaged electron density ne is 5.5×1019m-3, the electron and ion temperatures are 5 keV and 2.8 keV, respectively. The magnetic field Bt is directed to be clockwise (top view), whereas the plasma current Ip is oriented to be counter-clockwise in the standard operation. Fig. 1 depicts the arrangement of the HL-2A device together with the installation positions of the main systems used in this work. In this study, the discharge of HL-2A is maintained in the closed divertor configuration with bottom single null. The single null configuration is formed at the beginning of the discharge

and sustained until the end of the discharge. The main parameters of the ELM control experiment are shown in Table I.

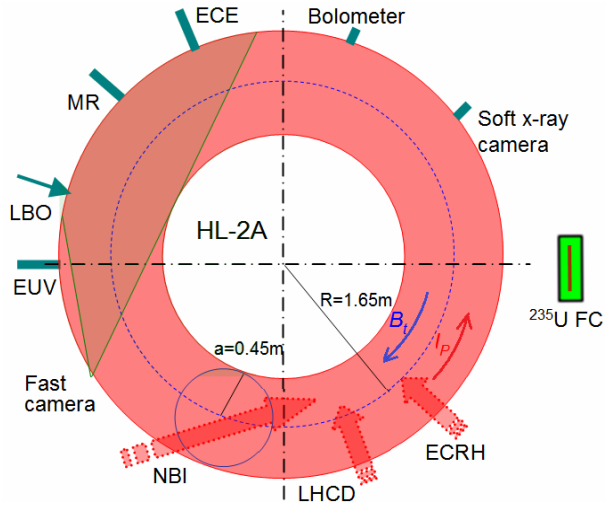

FIG. 1. Arrangement of the installation positions of the main systems used in this experiment.

TABLE 1. Main parameters in the ELM control experiment in HL-2A.

Plasma current, I_p	*150-200 kA*
Central line-averaged electron density, n_e	(1-3) $\times 10^{19}$m^{-3}
Central electron temperature, T_e	1-2 keV
Toroidal magnetic field, B_t	1.3 T
Plasma edge safety factor, q_{95}	4.0-6.0
Effective ionic charge, Z_{eff}	2.0-3.0
LBO injection impurity	Al, Fe, W
NBI power and pulse width	0.8-1.2 MW, 500 ms
ECRH power and pulse width	1.0-1.5 MW, 400 ms

Three auxiliary heating and current drive systems have been developed for HL-2A as follows: (1) electron cyclotron resonance heating (ECRH), consisting of six gyrotrons with the working frequency of 68 GHz, operates in the ordinary mode for delivering 3 MW (6 × 0.5 MW) power with 1 s pulse length; (2) neutral beam injection (NBI), including four positive-ion sources; the beam injection energy is typically 40 keV and a total beam power of up to 2.0 MW (4× 0.5 MW) is delivered for 2 s, and the neutral beam is tangentially co-injected into plasma; (3) lower hybrid current drive (LHCD), consisting of a passive-active multi-junction (PAM) launcher with the working frequency of 3.7 GHz; the peak parallel refractive index n//0 is 2.75 and the available power is 1.0 MW for 1s. The total output power of the auxiliary heating and current drive systems in HL-2A is about 6.0 MW.

A laser blow-off (LBO) impurity injection system has been built for HL-2A [13]. This system is installed on the equatorial-plane port and the impurities are vertically injected into plasma, as shown in fig. 1. A YAG laser with a pulse length of 10 ns and the wavelength of 1064 nm is employed for the LBO system. Its energy can reach up to 2 J. The target metal material is deposited onto a 42 mm × 42 mm × 2 mm quartz substrate with the thickness of several microns. The target plate is placed inside a vacuum tube located at the mid-plane diagnostic port of HL-2A, of which the position is approximately 710 mm away from the plasma boundary. The diameter of the LBO laser spot can be changed in the range of 2-6 mm. The LBO system has particular advantages for impurity injection: (1) well-controlled injected particle quantity; (2) localized deposition of the injected particles; (3) precise control of injection time. Several experiments exploited LBO to study impurity transport, as described for example in [14]. ELM control, resulting from impurity particle penetration into the pedestal region by LBO, has been realized for the first time in HL-2A. In this experiment, three kinds of metal impurities (Al, Fe, W) were injected into the ELMy H-mode plasma. Impurity related information is obtained from the detection of

emission of injected impurity particles located in different spatial regions. Line emission is measured by an extreme ultraviolet (EUV) spectrometer [15] and Dα detection arrays. Soft X-ray emission is detected by soft X-ray cameras with 25 μm Beryllium (Be) filters. Plasma global radiation is measured by bolometric arrays. In addition, a new high-speed visible light camera system has been developed recently. The camera frame rate using full pixel (1280 × 800) can be up to 7500 fps. Therefore, the camera system can provide some information about the LBO injected impurities with high spatio-temporal resolution.

Three fuelling tools can be used to control the density profile: gas puffing (GP) from the low-/high- field side (LFS/HFS), SMBI from the LFS and HFS, and pellet injection (PI) from the LFS mid-plane. SMBI is an efficient fuelling method which is considered to be an improvement over conventional GP. The electron density profile is measured with an eight-chord HCN laser interferometer (λ= 337 μm) [16] in the central region of the plasma ($\rho < 0.6$) and the edge density profile is measured with frequency modulated continuous microwave reflectometers (MR). The ion temperature is measured by a charge exchange recombination spectroscopy (CXRS) with 32 channels. The detection of the D-D fusion neutron emission rate is performed by a 235U fission chamber (FC) with uranium oxide of 3 g.

3. EXPERIMENTAL RESULTS

ELM control by actively injected impurity with LBO was performed and studied in order to verify the above-mentioned scenarios. In this experiment, three kinds of metal impurities (aluminum (Al), iron (Fe), tungsten (W)) with different atomic numbers were separately injected into the ELMy H-mode plasma. Both mitigation and suppression of ELMs have been successfully achieved by the LBO-seeded impurity. In the following the results of this experiment will be described in detail.

3.1. ELM mitigation by LBO-seeded impurity

The quantity of impurities injected by LBO can be flexibly adjusted by varying the diameter of the laser beam. ELM mitigation is achieved by injecting Fe and Al impurities. A typical ELM mitigation discharge by LBO-seeded Fe impurity is shown in Fig. 2. The plasma current and the toroidal magnetic field are 160 kA and 1.32 T, respectively. The ELMy H-mode is realized with 0.5 MW LHCD and 0.9 MW NBI. During the ELMy H-mode phase, the LBO system is triggered at 900 ms to start injecting Fe impurity into the plasma. At ~ 903 ms, the soft X-ray emission intensity (Fig. 2(b)) and the plasma radiation power (Fig. 2(e)) increase significantly, and there is a slight increase in the electron density (Fig. 2(a)). These observations indicate that the LBO-seeded impurity has entered in the plasma at this time.

Fig. 2(c) is the divertor Dα signal, it can be observed that there is a clear difference in the ELM frequency and ELM amplitude before and after LBO. The ELM frequency increases while the ELM amplitude decreases, implying that ELMs are effectively mitigated. The shaded area in Fig. 2 represents the time interval in which ELMs are mitigated, i.e. the duration of the LBO-seeded impurity influence. The impurity influence should not be constant during the whole mitigation phase. The seeded impurity profile can be calculated with data from bolometer array. As shown in Fig.9, the influence time of LBO-seeded impurity, which corresponds to the ELM mitigation phase, is much longer than the impurity concentration life time. Fig. 2 (d) and (f) represent the H98y2 factor and the plasma inner stored energy, respectively. From these figures, it can be observed that both the H98y2 factor and the plasma inner stored energy are almost unchanged by LBO-seeded impurity during the LBO influence phase. These indicate that the plasma confinement is not degraded and still in the high confinement state. Thus, the ELM mitigation by LBO-seeded impurity can be successfully achieved. The ELM mitigation terminates at t = 927 ms when ELM bursts restored to the state before the injection of the LBO-seeded impurity.

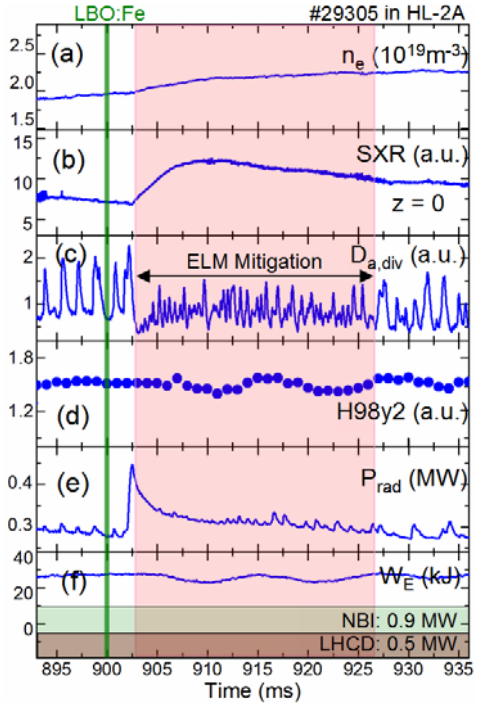

FIG. 2. Time evolution of the main parameters of a typical ELMy H-mode discharge with ELM mitigation by LBO-seeded Fe impurity. (a) Central line-averaged electron density. (b) Soft X-ray radiation intensity. (c) Divertor Da signal. (d) H98y2 factor. (e) Total plasma radiation power. (f) Plasma inner stored energy, LHCD and NBI monitors.

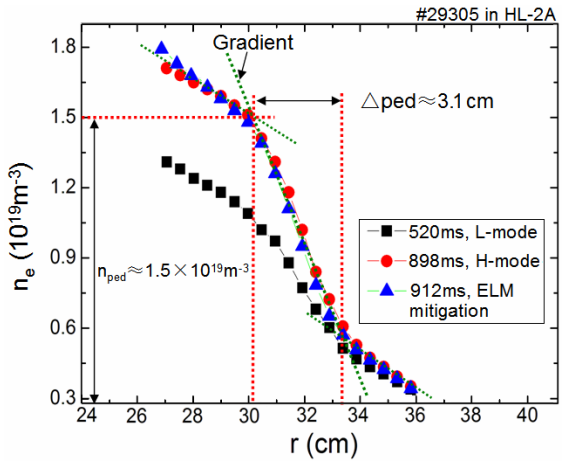

FIG. 3. Density profiles for the L-mode, H-mode and ELM mitigation phases.

Fig. 3 displays the density profiles measured by the microwave reflectometry during the L-mode (520 ms), ELMy H-mode (898 ms) and ELM mitigation (912 ms) phases. From this figure, a clear density pedestal structure can be identified during both ELMy H-mode and ELM mitigation phases. The top and foot of the pedestal structure are located approximately at r = 30.2 cm and r = 33.3 cm, respectively. Therefore, the width (△ped) of the pedestal is about 3.1 cm. In addition, the height (nped) of the pedestal is 1.5×1019m-3. The density pedestal structure during the ELM mitigation phase is exactly the same than that during the ELM phase. This means that the pedestal structure is still intact as before the ELM mitigation phase. Thus, the plasma during ELM mitigation is still in the high confinement state, which is consistent with the results of the H98y2 factor and the plasma inner stored energy.

Information on the location of the LBO-seeded impurity can be obtained by a bolometer array and a fast visible camera. The plasma radiation power density profile has been measured with the bolometer array. Fig. 4(d)

displays time evolution of the plasma radiation power density radial profile for shot 29305. From this figure, it can be seen that the clear image of the LBO-seeded impurity in plasma appears at about 903 ms and lasts for about 7 ms. The LBO-seeded impurity particles penetrate the edge plasma and are mainly deposited in the pedestal region, as shown in Fig. 4(d). A more intuitive process of LBO-seeded impurity injection for ELM mitigation can be observed by a fast visible camera, as shown in Fig. 5. The frame rate and the pixel of the camera are set by 10 kfps and 512 × 512, respectively. Therefore, the camera system can provide some information about the LBO-seeded impurities with high spatio-temporal resolution. The sequence of the images in Fig.5 is presented for the time points (t1, t2, …, t6) marked by an arrow in Fig. 4. The LBO system is triggered at 900 ms. Image t2 is the first frame picture with impurity appearing, which indicates that the total time of LBO response time and the impurity propagation time from the substrate to the plasma is about 2.8 ms. Image t5 is the last frame picture with impurity appearing. Thus, the injection of the LBO-seeded impurity into the plasma lasts about 7 ms. The images are coupled with the magnetic configuration reconstruction obtained by the EFIT code. EFIT reconstructions can provide important information on the evolution of the plasma configuration. From Fig. 5, it can be clearly observed that the LBO-seeded impurity is deposited mainly at the plasma edge. The measurement of the visible camera is consistent with the results of the bolometer array.

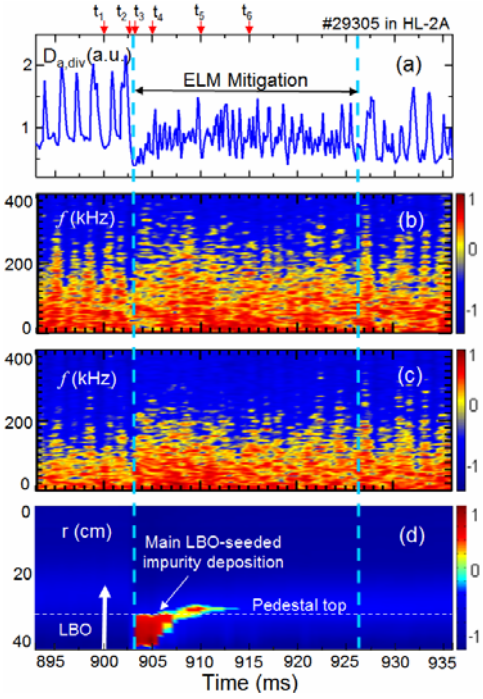

FIG. 4. Experimental results of ELM mitigation using LBO-seeded Fe impurity. (a) is the divertor Da signal, and the time interval of ELM mitigation is indicated by the double vertical dashed lines. (b) and (c) are the density fluctuation power spectra in the pedestal top and pedestal foot, respectively. (d) is the plasma radiation power density measured with the bolometer array.

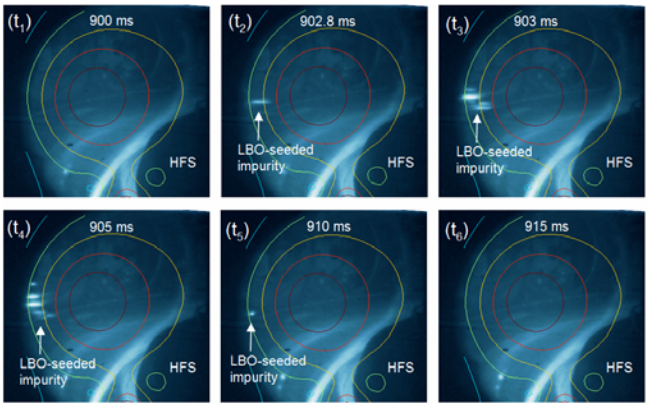

FIG. 5. Observations of the process of the LBO-seeded impurity injection for ELM mitigation by a fast visible camera.

3.2. ELM suppression and HCM excitation by LBO-seeded impurity

ELM suppression has been achieved by injecting LBO-seeded W impurity with higher atomic number. W is a promising divertor material for future magnetic fusion devices like ITER because its unique advantages, such as high melting point, low sputtering yield, and low tritium absorption. Thus, intense research activities have been conducted during the last few years on W impurity [17,18]. The ELMy H-mode is realized at 830 ms with 0.5 MW LHCD and 0.9 MW NBI. The LBO system is triggered to start injecting W impurity into the ELMy plasma. A transition from ELM mitigation to ELM suppression occurs after a further decrease in the divertor Dα signal, when the bursts of the divertor Dα signal completely disappear.

To study the transition process from ELM mitigation to ELM suppression, the information about the density fluctuation and the LBO-seeded impurity before and after this event is obtained, as shown in Fig. 6 by the dotted lines. Fig. 6(a) is the divertor D signal and the ELM suppression phase is noted by the double arrows. Fig. 6(b) and Fig. 6(c) show, respectively, the time evolution of the density fluctuation power spectra in the pedestal top and foot, which are measured by the reflectometry. Fig. 6(d) is the plasma radiation power density measured with a bolometer array. From these figures, a physical picture of the process can be inferred as the following. (1) Phase I: the LBO system is triggered at 900 ms during ELMy H-mode phase. (2) Phase II: the LBO-seeded W impurity enters the ELMy H-mode plasma at ~ 903 ms, and then the density fluctuations are enhanced and ELMs are effectively mitigated. The turbulence behavior during this phase is the same as that during LBO-seeded Fe impurity ELM mitigation. The duration of this phase is very short. (3) Phase III: during this phase, ELMs are completely suppressed, and more surprisingly, the pedestal turbulence measured by the Doppler reflectometry is also nearly suppressed as shown in Fig. 6(b) and Fig.6(c). From Fig. 6(d), it can be observed that the power density of plasma radiation becomes stronger gradually, implying that more and more impurities entering the plasma. This indicates that the ELM mitigation- suppression transition strongly correlates with the increasing of LBO-seeded impurities entering the plasma. It suggests that the ELM mitigation- suppression transition may be triggered when the amount of the LBO-seeded impurities entering the plasma exceeds a certain threshold value.

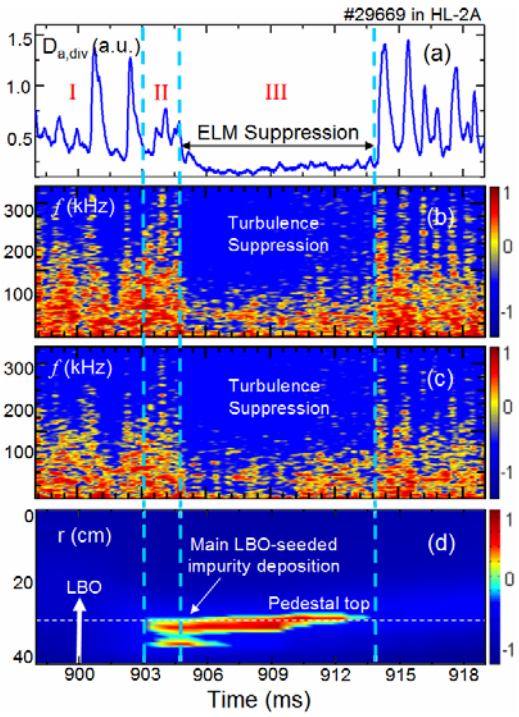

FIG. 6. Experimental results of ELM suppression using LBO-seeded impurity. (a) is the divertor Da signal. (b) and (c) are the density fluctuation power spectra in pedestal top and pedestal foot, respectively. (d) is the plasma radiation power density.

Fig. 6(b) and (c) show the time evolution of the density fluctuation power spectra in the pedestal top and foot, respectively. The pedestal density fluctuations are enhanced during ELM mitigation phase, as previously described. During ELM suppression phase, the pedestal density fluctuations are nearly suppressed. However, the

analysis of the magnetic signal has shown that a harmonic coherent mode (HCM) is excited during this ELM suppression phase as shown in Fig.7, where Fig. 7(a) presents the divertor Dα signal, Fig. 7(b) is the magnetic probe signal measured by Mirnov coil, Fig.7(c) presents the time-frequency spectrum of the magnetic fluctuations, and the two dashed lines delimit the ELM suppression interval. The frequency range of HCM is from 10 to 100 kHz. During this phase, as the pedestal turbulence is nearly suppressed, the base line of the divertor Dα signal is significantly reduced, and the plasma density continuously increases. This HCM is very similar to that observed in EAST, where a harmonic coherent mode is spontaneously excited during an ELM suppression phase [19]. Furthermore, it has been found that strong interaction exists between different harmonics of HCM and background turbulence, and energy transfer can be transferred from the background turbulence to HCM. This could explain the reduction of the pedestal turbulence and the enhancement of the particle confinement with HCM. Similarities exist between HCM and the edge harmonic oscillation (EHO) observed during the Quiescent H-mode plasmas in the DIII-D tokamak [20], for example, the spatial location, the fundamental frequency, and the multiple harmonic features. However, the impact of EHO on the plasma is quite different to that of HCM. EHO modulates the pedestal turbulence, regulates the particle transport, suppresses ELMs, and maintains the plasma for a steady state [21,22], while HCM suppresses the pedestal turbulence, reduces the particle transport, and raises the plasma density. These suggest that HCM could extend the Peeling-Ballooning instability limit for ELM triggering, as predicted by theory [23]. As shown by the present experiments, HCM can not only be spontaneously excited in H-mode plasmas, but also externally excited with impurity seeding. In the future our effort will focus on the investigation of the excitation mechanism of HCM.

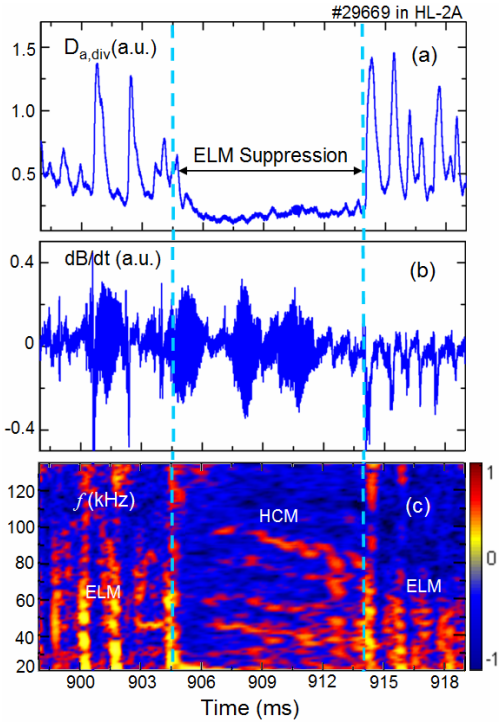

FIG. 7. Observation of the harmonic coherent mode (HCM) during the ELM suppression phase. (a) Divertor Da signal. (b) Magnetic probe signal measured by the Mirnov coil. (c) Time-frequency spectrum of the magnetic fluctuation signal.

4. CONCLUSIONS

ELM control has been achieved in HL-2A with LBO-seeded Al, Fe and W impurities. The transition process from ELM mitigation to ELM suppression has been clearly observed. The transition is triggered when the amount of the LBO-seeded impurity exceeds a certain threshold value. The pedestal density fluctuation is significantly reduced during ELM suppression phase, and a harmonic coherent mode is excited, implying that ELM suppression is associated with the onset of HCM triggered by LBO seeded impurity, and suggesting that HCM could extend the Peeling-Ballooning instability limit, as predicted by the theory. This regime in ELM suppression plasma is different to the recent ELM-free H-mode in HL-2A. The dependence of the ELM

mitigation and suppression on the LBO laser spot diameter has been demonstrated, indicating the quantity of electrons injected with impurity is likely the key parameter for controlling ELMs.

ACKNOWLEDGEMENTS

This work was partially supported by the National Science and Technology Major Project of the Ministry of Science and Technology of China (Grant Nos. 2014GB109003 and 2015GB111002), the National Natural Science Foundation of China (Grant Nos. 11775068 and 11375004), and it was also partially supported within the framework of the cooperation between the French Commissariat a l'Energie Atomique et aux Energies Alternatives (CEA) and the China National Nuclear Corporation (CNNC).

REFERENCES

[1] Lang P.T. et al 2013 Nucl. Fusion 53 043004
[2] Evans T.E. et al 2004 Phys. Rev. Lett. 92 235003
[3] Suttrop W. et al 2011 Phys. Rev. Lett. 106 225004
[4] Jeon Y.M. et al 2012 Phys. Rev. Lett. 109 035004
[5] Liang Y. et al 2013 Nucl. Fusion 53 073036
[6] Kim J. et al 2017 Nucl. Fusion 57 022001
[7] Xiao W.W. et al 2014 Nucl. Fusion 54 023003
[8] Lang P.T. et al 2015 Plasma Phys. Control Fusion 57 045011
[9] Lang P.T. et al 2004 Plasma Phys. Control. Fusion 46 L31
[10] Li J et al 2013 Nature Phys. 9 817
[11] Chen R. et al 2015 Nucl. Fusion 55 033012
[12] Xu M. et al 2015 Nucl. Fusion 55 104022
[13] Cui Z.Y. et al 2013 Nucl. Fusion 53 093001
[14] Valovi˘c M. et al 2013 Plasma Phys. Control. Fusion 55 025009
[15] Cui Z.Y. et al 2014 Rev. Sci. Instrm. 85 11E426
[16] Zhou Y. et al 2007 Rev. Sci. Instrum. 78 113503
[17] Murakami I. et al 2015 Nucl. Fusion 55 093016
[18] Angioni C. et al 2014 Nucl. Fusion 54 083028
[19] Zhou C. et al. 2017 submitted to Nucl. Fusion
[20] Greenfield C. M. et al. 2001 Phys. Rev. Lett. 86 4544
[21] Suttrop W. et al. 2003 Plasma Phys. Control. Fusion 45 1399
[22] Oyama N. et al. 2005 Nucl. Fusion 45 871
[23] Xi P.W., Xu X.Q., Diamond P.H., 2014 Phys. Rev. Lett. 112 085001